SMALL WOOD PELLET BOILER 3-D CFD STUDY FOR IMPROVED FLUE GAS EMISSIONS EMPLOYING FLUE GAS RECIRCULATION AND AIR STAGING

by

Filip KOKALJ[a*], Tomas ZADRAVEC[a], Aleksandar M. JOVOVIĆ[b], and Niko SAMEC[a]

[a] Faculty of Mechanical Engineering, University of Maribor, Maribor, Slovenia
[b] Faculty of Mechanical Engineering, University of Belgrade, Belgrade, Serbia

Original scientific paper
https://doi.org/10.2298/TSCI2301089K

Wood biomass fuels have become increasingly important in terms of achieving future sustainability targets regarding RES, especially to reduce GHG and the use of domestic energy sources, on other hand with these fuels the pulutant air emissions have to be addressed with great attention. Nowadays, air staging and flue gas recirculation are often used as a primary emission reduction measure in large scale biomass fuel fired boilers, but their combined application in small scale commercial wood pellet boilers is not so common. The implementation of this approach to the small scale burning devices can enable further development of small boilers, in order to achieve a more complete combustion and reduction of pollutant emissions, especially CO, NO_x, and PM. In the presented work a comprehensive numerical and experimental study on the combustion parameters is performed, in order to determine the overall combustion properties. A commercial 32 kW small-scale hot water wood pellet boiler was modified numerically from the operating point of view. The findings of this study, like different combinations of recirculated flue gases and secondary air amount, can serve as useful guidelines for the new innovative design and optimisation of the air and recirculated flue gas injection process parameters. The scenarios of this study, where recirculated flue gas was added to the secondary air, were beneficial. Optimally, a CO reduction of 63% was achieved by adding 30% of recirculated flue gas to the secondary air stream, and a 22% reduction was achieved for the NO emissions.

Key words: *CFD, combustion, wood pellets, air staging, flue gas recirculation*

Introduction

Due to the comparatively high costs of the secondary measures, only primary emission reduction techniques are practical for small-scale biomass boilers [1]. Solid biomass fuels can be burned more completely with air staging, which is regarded as a key primary emission reduction strategy, since it increases combustion efficiency and reduces emissions [2]. The basic air staging principle is presented in fig. 1. In the first stage, primary air (PA) is added for the devolatilisation and gasification of the solid fuel. In the second stage, sufficient secondary air (SA) is added to ensure complete combustion. The control of mixing, temperature, O_2 concentration and residence time enables combustion with low emissions at the highest efficiency [3].

* Corresponding author, e-mail: filip.kokalj@um.si

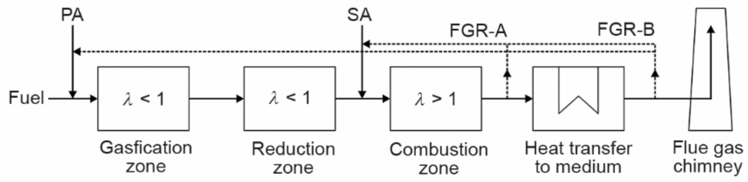

Figure 1. Air staging combustion principle with flue gas recirculation, based on [4]

The composition of the gas flow above the fuel bed is very heterogeneous, and almost the same composition can extend past the SA inlets in small-scale systems due to poor mixing and flow turbulence [5]. Because the SA parameters have a substantial influence on turbulence, and, as a result, on the mixing of volatiles with air, their function in creating a good air staging is significant. Several research efforts showed the effect of the SA parameters on air staging effectiveness. For example, Zdravec *et al.* [6] demonstrated that the temperature of SA entering the combustion chamber effects the CO emissions considerably. Furthermore, the CO emissions were affected by the direction, velocity and temperature profile of each separate SA nozzle. Khodaei *et al.* [7] found that a 50% reduction of CO emissions and a nine fold reduction of PM emissions can be achieved with air staging, by deploying a uniform SA module in a higher position from the bed in an experimental pellet burner.

Flue gas recirculation (FGR) is not common in small-scale furnaces. Several process parameters that affect the air staging strategy can be influenced by adding a stream of recirculated flue gases (RFG) to the SA stream. For example:

– The excess air ratio in the secondary combustion zone can be altered.
– The global excess air can be lowered owing to increased mixing rates in the secondary combustion chamber.
– The SA stream can be preheated.
– The temperature of the walls of the SA manifold can be elevated.
– The velocity of the SA streams can be accelerated to enhance the range of the oxygen rich stream into the reactive zone and to enhance mixing.

Additionally, internal flue gas recirculation (IFGR) in the combustion chamber can be promoted with the application of FGR.

The properties of the RFG stream added to the combustion chamber depend greatly on the location of its extraction. As seen in fig. 1, the RFG stream can be extracted at several locations of the boiler. For example, if extracted at the FG outlet, its properties will be that of the final products, which are composed mainly of CO_2, N_2, O_2, and H_2O, while having a temperature between 100-150 °C. On the other hand, the RFG stream can be extracted alternatively from a different location in the boiler. For example, if the RFG are extracted before the heat exchanger, its composition and temperature can differ vastly from the end of the boiler flue gas composition and temperature.

To the authors' knowledge there are no research efforts presented which would investigate the impact of the different properties of the RFG stream on the combustion process in small scale biomass combustion. Therefore, the aim of the present research is to explore the characteristics of the FGR and air staging combustion concept of a commercial, residential-scale wood-pellet hot-water boiler. By computing several different cases the effect of the 10 wt.%, 20 wt.%, and 30 wt.% RFG addition (*i.e.*, the percentage of the total flue gas mass-flow) to the SA stream is investigated on the emissions of CO and NO with a fixed air staging strategy (*i.e.*, a fixed PA/SA ratio). Furthermore, the impact of the temperature of the RFG stream is investigated by testing three different temperatures of the RFG stream. In addition, the impact of FGR on the IFGR is studied, as there are no such studies conducted, which poses an interesting novelty.

Properties of the combustion device

The boiler is made up of two parts: a combustion chamber, which includes the underfed fixed-grate in its bottom portion, and a heat exchanger made up of two passages, two sets of bundles of fire tubes, and turning chambers that are both completely water-cooled. The grate is suspended in the center of the combustion chamber by the fuel supply line. Fresh wood pellets are pushed through the center of the circular fixed grate from below, and then travel radially towards the grate's outer perimeter. There are several small holes (4-5 mm) located on the grate that allow the PA to enter the fuel bed from below. More information on the boiler's geometry is provided in [6, 8].

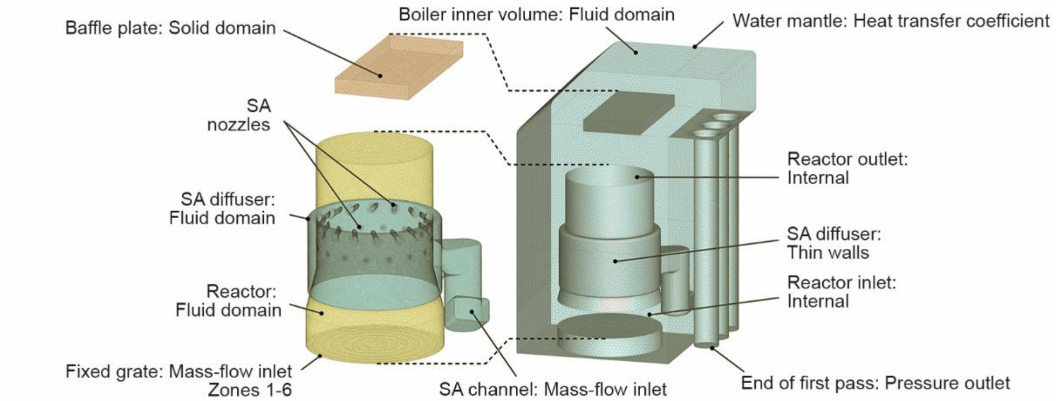

Figure 2. Geometry of the computational domain with the main features

A stepwise fuel feeding profile results in the formation of a fuel bed that is essentially static, and whose characteristics do not change considerably over time. Fresh fuel burns entirely while moving across the grate. The leftover ash is ejected from the grate's edge. Gaseous products pass through the SA supply diffuser, which has 16 upper tube nozzles with a diameter of 8 mm and 16 lower openings with a diameter of 6 mm, fig. 2. When the SA is added, the reactants are mixed vigorously at a high enough air excess to oxidize the reacting gas mixture completely. The products move via the heat exchanger and into the chimney before exiting through the exhaust fan.

Properties of the high-grade wood pellets

High quality wood pellets were employed in the experimental investigation. Following the results from the proximate and ultimate analyses, performed in line with EN ISO 17225-2 and CEN/TS 16023, the fuel can be classified as high grade, *i.e.*, A1 grade. Because of the low ash content and moisture, the higher heating value (HHV) of the fuel was 18.989 MJ/kg, while the lower heating value (LHV) was 17.928 MJ/kg. The cylindrical wood pellet particles were of various lengths between 4 to 32 mm, while their diameter was 6 mm. The fuel specific characteristics are gathered in tab. 1.

Table 1. Properties of the used fuel

Ultimate analysis (daf) [wt.%]				Proximate analysis (ar) [wt.%]			
C	H	N	O	VM	FC	A	M
47.30	5.31	0.54	46.85	83.86	10.22	0.37	5.55

The CFD combustion simulation approach

The CFD simulation approach employed in this study was based on a previously established and verified CFD modelling strategy for the prediction of solid fuel combustion in a residential-scale wood-pellet hot-water boiler [6]. An empirical 1-D fuel bed combustion model was used to represent the solid fuel conversion process, which was based on the measured operating parameters, fuel characteristics, and solid fuel conversion parameters process, based on observation.

Concentric wood pellet combustion model

The grate is separated into six concentric regions, Z1-Z6, fig. 3. The zones correspond to certain areas of the grate, to enhance the accuracy of the boundary conditions. For instance, zones Z1 and Z2 overlay the fuel supply orifice, while zones Z4, Z5 and Z6 overlay the region of PA inflow holes. The distribution of PA across the grate is determined primarily by the number and diameter of the holes coincident with each zone and the measured PA flow through the inlet holes and infiltration air (IA) flow through the fuel supply, and is defined by two air distribution parameters: $\beta_{\mathrm{PA,i}}$ and $\beta_{\mathrm{IA,i}}$. The fuel conversion parameters; $\beta_{\mathrm{FC,i}}$, $\beta_{\mathrm{VM,i}}$, and $\beta_{\mathrm{M,i}}$ define the intensities of the fixed carbon (FC) oxidation, volatile matter (VM) and moisture (M) release processes in each zone, respectively. Table 2 shows the specified fuel conversion and PA and IA distribution parameters.

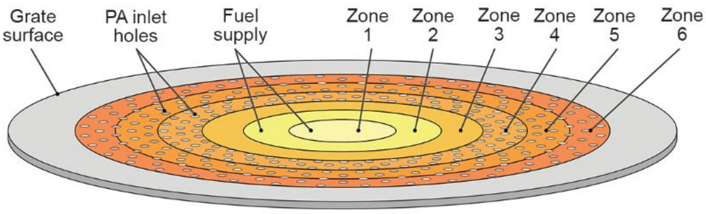

Figure 3. The cylindrical grate with zone placement

During the drying process all moisture is emitted completely from the fuel bed as water vapour. The VM produced during devolatilisation is approximated by a synthetic molecule $C_1H_{1.699}O_{0.965}$ with a molecular weight of 29.169 kg/kmol and a formation enthalpy of –9.158·10^7 J/kmol. The fuel-N is assumed to be emitted from the bed as NH_3. The FC reacts with O_2 into CO and CO_2. The ratio of CO to CO_2 is temperature dependent [6]. This process is exothermic, and this generates heat.

During the experimental trial the fuel bed was observed visually to determine the fuel conversion coefficients. The percentage of the fuel transformation sub-process that takes place in each zone is effectively represented by the fuel conversion coefficients. The distribution of air flow between the grate zones is influenced by the grate's design, as well as the experimentally determined PA and IA.

Table 2. Chosen parameters for the fuel bed and air inflow

Fuel conversion parameters [%], PA and IA distribution parameters [%]							
Concentric grate zone	Z1	Z2	Z3	Z4	Z5	Z6	$\Sigma\beta_{r.i}$
Drying, $\beta_{M.i}$	30.0	50.0	20.0	–	–	–	1
Devolatilisation, $\beta_{VM.i}$	5.0	7.5	10.0	52.5	25.0	–	1
Char oxidation, $\beta_{FC.i}$	–	–	20.0	27.0	38.0	15.0	1
PA inflow, $\beta_{PA.i}$	–	–	20.0	31.0	23.0	26.0	1
IA inflow, $\beta_{IA.i}$	30.0	50.0	20.0	–	–	–	1

Gas phase combustion model

The fuel bed model's projected flammable gas mixture, made up of H_2O, $C_1H_{1.699}O_{0.965}$, CO, CO_2, NH_3, N_2, and O_2, flows into the computational domain perpendicular with respect to the grate. According to [9], the intake turbulence intensity and length scale were adjusted to 35% and 0.004 m for all considered scenarios. A two-step global reaction scheme with volatile species and CO oxidation was used to simulate the homogeneous combustion. The basic reaction scheme, taken from [10], was enhanced by the NH_3 conversion into N_2 and H_2O by a pair of reactions with NO as the intermediate. Reactions R3 and R4 were taken from [11], while their rates were taken from [12]. The eddy-dissipation model (EDM) and finite-rate (FR) were used for the solution of the volumetric chemical reactions.

$$C_1H_{1.699}O_{0.965} + 0.442O_2 \rightarrow CO + 0.849H_2O \tag{1}$$

$$CO + 0.5O_2 \rightarrow CO_2 \tag{2}$$

$$NH_3 + O_2 \rightarrow NO + H_2O + 0.5H_2 \tag{3}$$

$$NH_3 + NO \rightarrow N_2 + H_2O + 0.5H_2 \tag{4}$$

$$r_1 = 5\cdot 10^{12} e^{-\frac{2\cdot 10^8}{RT}} [C_1H_{1.699}O_{0.965}]^{0.2}[O_2]^{1.3} \tag{5}$$

$$r_2 = 2.239\cdot 10^{12} e^{-\frac{1.702\cdot 10^8}{RT}} [CO][O_2]^{0.25}[H_2O]^{0.5} \tag{6}$$

$$r_3 = 4\cdot 10^{6} e^{-\frac{1.34\cdot 10^5}{RT}} [NH_3][O_2]^{0.5}[H_2]^{0.5} \tag{7}$$

$$r_4 = 1.80\cdot 10^{6} e^{-\frac{1.13\cdot 10^5}{RT}} [NH_3][NO] \tag{8}$$

The gas mixture density was calculated using the incompressible ideal gas law, the specific heat was determined by the mixing law, the thermal conductivity was set to constant 0.0454 W/mK, and, similarly, a constant viscosity of $1.72\cdot 10^{-5}$ kg/ms was used. All other gas parameters were left as default by the ANSYS FLUENT version 2021 R2.

The 3-D numerical modelling in the freeboard region

The ANSYS FLUENT version 2021 R2 was used to solve the gas phase combustion CFD problems. All different numerical problems were resolved using the SIMPLE approach for the pressure-velocity coupling. Turbulence was simulated using the realisable k-ε model, enhanced wall functions and default constants [13]. All equations were discretised in the 2nd order spatially.

Several fluid and a solid domain made up the mesh, fig. 2. It was possible to simulate the SA flow from the intake to all 32 nozzles by building the SA diffuser with thin walls that had the properties of 2 mm thick sheet steel. Heat transfer through the thin walls was made possible through the thermal coupling of the walls and shell conduction. As a result, the distribution of the SA flow and temperature was simulated actively. The baffle plate conducted heat through coupling with the fluid domain.

The numerical mesh was constructed of $2.65 \cdot 10^6$ volume cells while having a minimum orthogonal mesh quality factor of 0.3. A mesh independence study was performed to achieve mesh independent results. The average size of the surface elements was studied for a particular region and the growth rate of the elements. Also, a sufficiently dense mesh size was built along the walls. Those parameters were made progressively smaller until there were no more significant changes in the results.

The flow near the wall was simulated with the k-ε turbulent flow model with enhanced wall treatment. Thus, it was necessary to provide a sufficiently dense mesh size along the walls to allow the correct prediction of the large gradients that are characteristic to the area along the wall. The parameters of this layer were adapted to the smooth transition between prisms and the volume grid. An inflated prism cell layer was added to all surfaces except the grate and outlet. This allowed for precise simulation of near wall flow and heat transfer. Given the complexity of the geometry, which a hexagonal element mesh cannot mesh easily, the majority of the grid was built from polyhedrons and polyhedral prisms. The geometry used in this study was the actual inner volume of the combustion chamber.

A convection boundary condition was used to model the walls that were cooled by water. The water cooled walls convective heat transfer coefficient was fixed at 2500 W/m^{2}K, and the temperature of the water's free stream was fixed at 70 °C. The boiler water-cooled walls' thickness was fixed at 5 mm. The adiabatic boundary conditions, which prevent heat flow, were used to simulate well insulated surfaces *e.g.*, lids and the boiler floor. Lastly, at the flue gas exhaust, a negative pressure of –10 Pa relative to the operational pressure was prescribed, which is typical for such systems in actual use.

The incident thermal radiation absorbed by the surface of the fuel, emitted by heated surfaces, glowing particles, and exothermic reactions, affects the fuel conversion model. Therefore, the radiative heat transfer was simulated using the discrete ordinates (DO) model. For a limited range of angles, the radiative heat transfer equation may be solved using the DO model. In this study, a 6 × 6 angular discretisation worked well. The weighted sum of grey gases domain-based model was used to compute the radiation absorption coefficient. All interior walls had an internal emissivity of 0.8 [14].

Air staging and flue gas recirculation scenarios

First, a numerical simulation was conducted with the fuel bed boundary conditions listed in tab. 2 and no FGR. This simulation was the baseline simulation with the designation R0. The boundary conditions of the air staged combustion for the baseline case simulation are listed in tab. 3. The air staging boundary conditions used for the baseline case were measured in the experimental campaign, and coincided with the normal operation at a nominal heat output of the system.

Table 3. Boundary condition for the baseline case R0 and its flue gas composition

Baseline case process parameters [gs^{-1}]		Flue gas composition [%], λ [–]	
Fuel supply, $\dot{m}_g$	1.961	CO_2	15.0
The PA mass-flow, $\dot{m}_{PA}$	7.452	Oxygen gas, O_2	11.0
The IA mass-flow, $\dot{m}_{IA}$	3.922	Water vapour, H_2O	5.0
The SA mass-flow, $\dot{m}_{SA}$	8.237	Nitrogen gas, N_2	69.0
Flue gas flow, $\dot{m}_{FG}$	21.572	Air excess, λ	2.054

From the case R0 the composition of flue gases was extracted, analysed, and its composition is listed in tab. 3. The parameters listed in tab. 3 are based on experimental measurements. The same composition was used for the parametric study of the impact of FGR on the combustion process. Nine cases were considered, varying in the temperature and percentage of RFG. For example, for cases R1T1, R1T2, R1T3, 10% of the total mass-flow of flue gases, $\dot{m}_{FG}$, was supplied to the SA flow. The RFG temperature of those cases was 398, 598, and 798 K, respectively. All other combinations of SA and RFG combinations are listed in tab. 4. The end composition and temperature of the perfectly mixed SA + RFG flow for all cases are also listed in tab. 4.

Table 4. Combinations of the considered flue gas recirculation parameters

Gas inlet mixture composition [%], mass-flow [gs^{-1}] and temperature [K]									
Numerical case	R1T1	R1T2	R1T3	R2T1	R2T2	R2T3	R3T1	R3T2	R3T3
The RFG amount	10			20			30		
The RFG temperature	398	598	798	398	598	798	398	598	798
Temperature, T_{SA+RFG}	319	360	402	332	401	470	342	430	518
CO_2	0.031			0.052			0.066		
Oxygen gas, O_2	0.203			0.187			0.176		
Water vapour, H_2O	0.017			0.022			0.027		
Nitrogen gas, N_2	0.749			0.739			0.731		
Mass-flow, $\dot{m}_{SA+RFG}$	10.353			12.507			14.661		

Results and discussion

First, the baseline case R0 results were validated against the measured values obtained during the experimental campaign. Then, the impact of FGR on the gaseous emissions was discussed by analysis of the results of the numerical parametric study.

Baseline simulation results

The baseline case R0 results were compared against the temperatures recorded at four measurement ports spaced throughout the combustion chamber. The measurement points were divided into three distinct areas:

– The primary combustion zone (P-CZ), situated directly above the grate and beneath the SA nozzles.
– The secondary combustion zone (S-CZ), situated immediately above the SA diffuser.

– The post-secondary combustion zone (PS-CZ), situated above the baffle plate. In addition, fig. 4 shows a comparison between the recorded and simulated vertical temperature profiles for the baseline case R0. The vertical profile was selected for the validation, as it captures the temperature profile of the combustion process under study reasonably well.

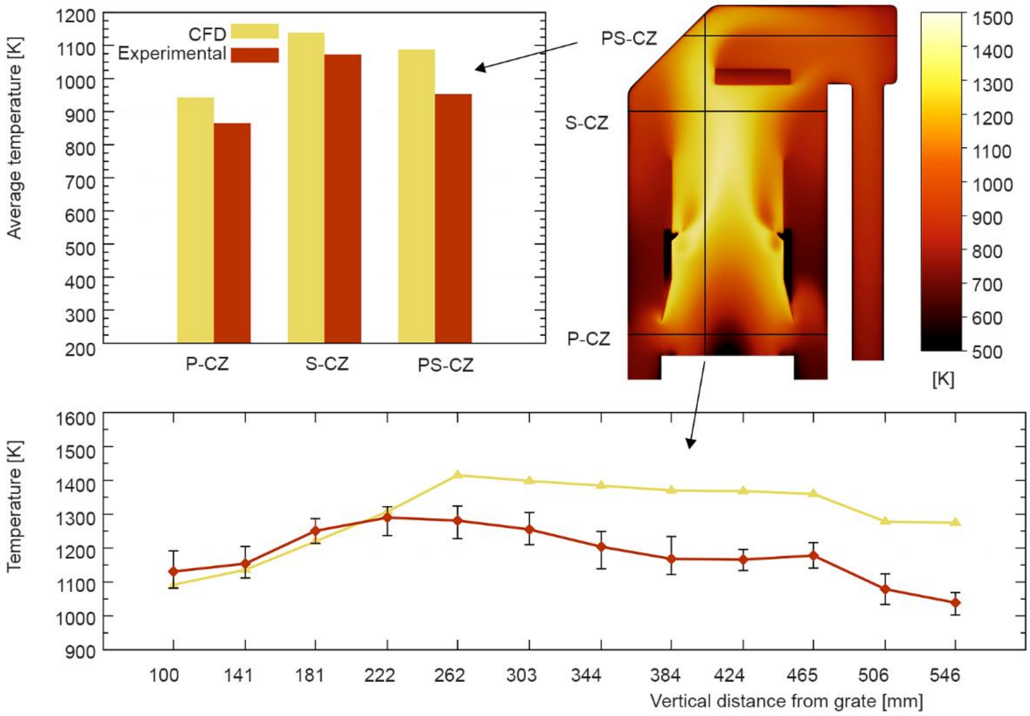

Figure 4. Experimental temperature validation of the CFD simulation results

The combustion temperatures were overpredicted considerably in the combustion chamber for the baseline case. Despite the significant simulation deviations from the values obtained experimentally, the simulated temperature field was of the correct shape, fig. 4. The overprediction can be attributed to both the simplified numerical approach and the experimental procedure. For instance, the modelling approach ignores the soot production. Therefore, the effect on the radiative heat flow from the soot laden flame, the interior walls and the fuel particles was not considered. Furthermore, because they are challenging to evaluate, heat losses from the fuel were not taken into consideration in this research.

Impact of flue gas recirculation on the gaseous emissions

The CFD predicted gaseous emissions are presented in fig. 5. As can be seen, the scenarios where RFG were added to the SA were beneficial in all cases regarding the CO and NO emissions. Optimally, a reduction of 63% was achieved by adding 30% of RFG to the SA stream at a combined temperature of 518 K. Similarly, a 22% reduction was achieved for the NO emissions. The concentration of CO and NO was expressed for dry flue gases at a normalised O_2 content of 10%. The predictions of the baseline case R0 lay in the measured range, and are representative for the observed boiler, except for the NO emissions which were over predicted moderately.

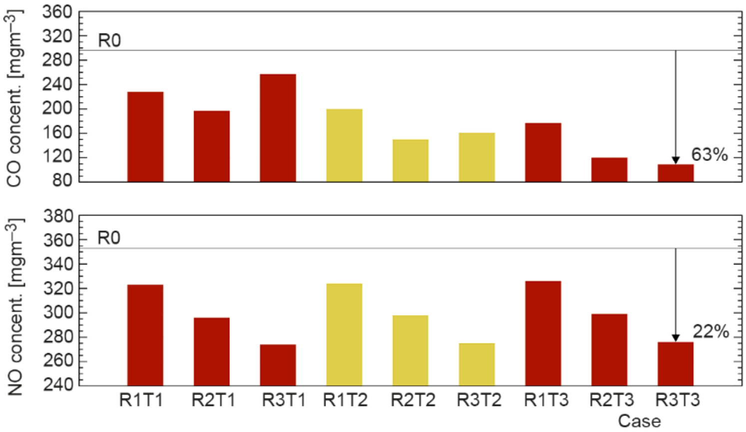

Figure 5. Predicted CO and NO emissions

As is observable in figs. 5 and 6 the CO emissions were lowered by elevated SA+RFG temperatures. This held true in all groups of constant FGR percentage (*e.g.*, cases R*x*T1, R*x*T2, R*x*T3). The lowest emissions were obtained by the strongest FGR strategy of 30% at the highest temperature of the RFG stream of 797 K, resulting in a mixture temperature of 518 K. A high RFG percentage and a low temperature, as prescribed in case R3T1, produced high CO emissions.

From fig. 6 it can be observed that the highest CO emission levels were predicted for the case R3T1, where the strongest flow of RFG was assumed at a mixture temperature of 342 K. Despite the large mass-flow, the relatively low SA + RFG temperature caused the reactive mixture to be under cooled, effectively lowering the reaction rates of CO oxidation to CO_2.

The combined effect of the RFG addition at an elevated temperature caused an increase in velocity at the SA nozzles, as can be seen in fig. 7. For case R3T3 the average velocity of gases leaving the 32 SA nozzles was effectively doubled compared to the baseline case R0. The higher velocity caused better mixing due to increased inlet turbulence. Furthermore, due to the higher velocities, considerably more oxidiser got transported to the central region of the SA diffuser, and thus improved the CO burnout.

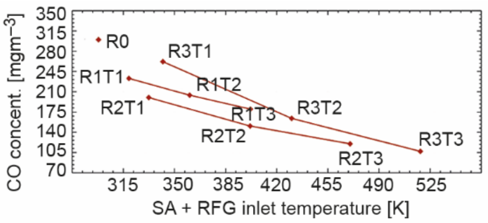

Figure 6. Correlations between the SA + RFG temperature and CO emissions

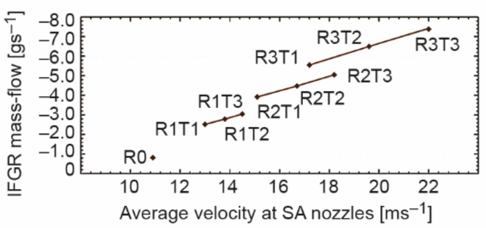

Figure 7. Correlations between the average velocity at the SA nozzles and the IFGR effect

The higher SA nozzle velocities caused an important effect to be facilitated, namely, the IFGR effect in the combustion chamber. Owing to the upward orientated SA nozzles, the elevated volume flow here caused a region of negative pressure relative to the boiler`s internal volume, which caused the gases near the outer circumference of the grate to be drawn into the SA diffuser. The magnitude of the IFGR was increased by almost eight-fold when employing FGR.

The highest value of the IFGR mass-flow was achieved by the case R3T3. The magnitude of the IFGR mass-flow seemed to correlate well with the average velocity at the SA nozzles. Both the FGR portion and the temperature of the SA+RFG mixture were related to the IFGR mass-flow linearly.

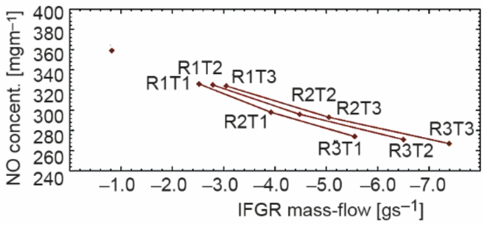

Figure 8. Correlations between the IFGR mass-flow and NO emissions

The NO emissions correlated to the IFGR mass-flow linearly for cases in the same temperature group (*e.g.*, cases R1T*x*, R2T*x*, R3T*x*), fig. 8. A slight decrease in NO concentration was observed for the change of temperature inside each group of fixed FGR ratio. This indicated that the inlet temperature of the SA+RFG mixture was less relevant for achieving low NO emissions than the amount of RFG. Again, the case R3T3 resulted in the lowest NO emissions.

The contours of temperature, volatiles` mass fraction, velocity, CO, CO_2, H_2, NH_3, NO, and O_2 concentrations at the frontal cross-section are presented in fig. 9. It is possible to observe that, in case R0, there were some streams of high temperature gases escaping from the SA diffuser around the outer circumference of the grate. Furthermore, a region of gas with a high CO content can be seen in the same location. Hence, it can be assumed that the flammable gases did not flow through the top of the SA injection region entirely, and that the flow of IFGR was not distributed completely uniformly around the grate. Although there was some outflow, the IFGR effect was still positive, meaning that, overall, gases were drawn into the SA diffuser.

The magnitude of the IFGR flow had an effect on the NO emission, as shown in fig. 8. This can also be observed in fig. 9 by considering the contours of the NO concentration. The flow of gases into the SA diffuser caused a change in the composition of the reactive flow in the primary combustion zone due to the influx of the almost complete combustion products of the secondary phase. Furthermore, the temperature of the reactive flow changed. Consequently, this modification of the primary zone combustion conditions cases caused a change in the reaction rates and residence times, and, thus, promoted the cutback of NO and reduced the rate of NO creation due to NH_3 oxidation. Furthermore, due to the IFGR, some NO and NH_3 was recirculated into the SA diffuser, and thus participated in the NO reduction reaction.

Conclusions

There are several important process parameters linked to the SA supply which impact the air staging strategy effectiveness in small scale biomass combustion. Several of the vital process parameters that affect the air staging strategy can be influenced by adding a stream of RFG to the SA stream in small scale biomass combustion. Therefore, the purpose of this work was to study the effect of the FGR method in conjunction with the air staging strategy on the combustion process efficiency and gaseous emissions in a small-scale wood pellet boiler.

The simulation methods employed in this study relied on the validated CFD modelling strategy for the prediction of solid fuel combustion in a residential-scale wood-pellet

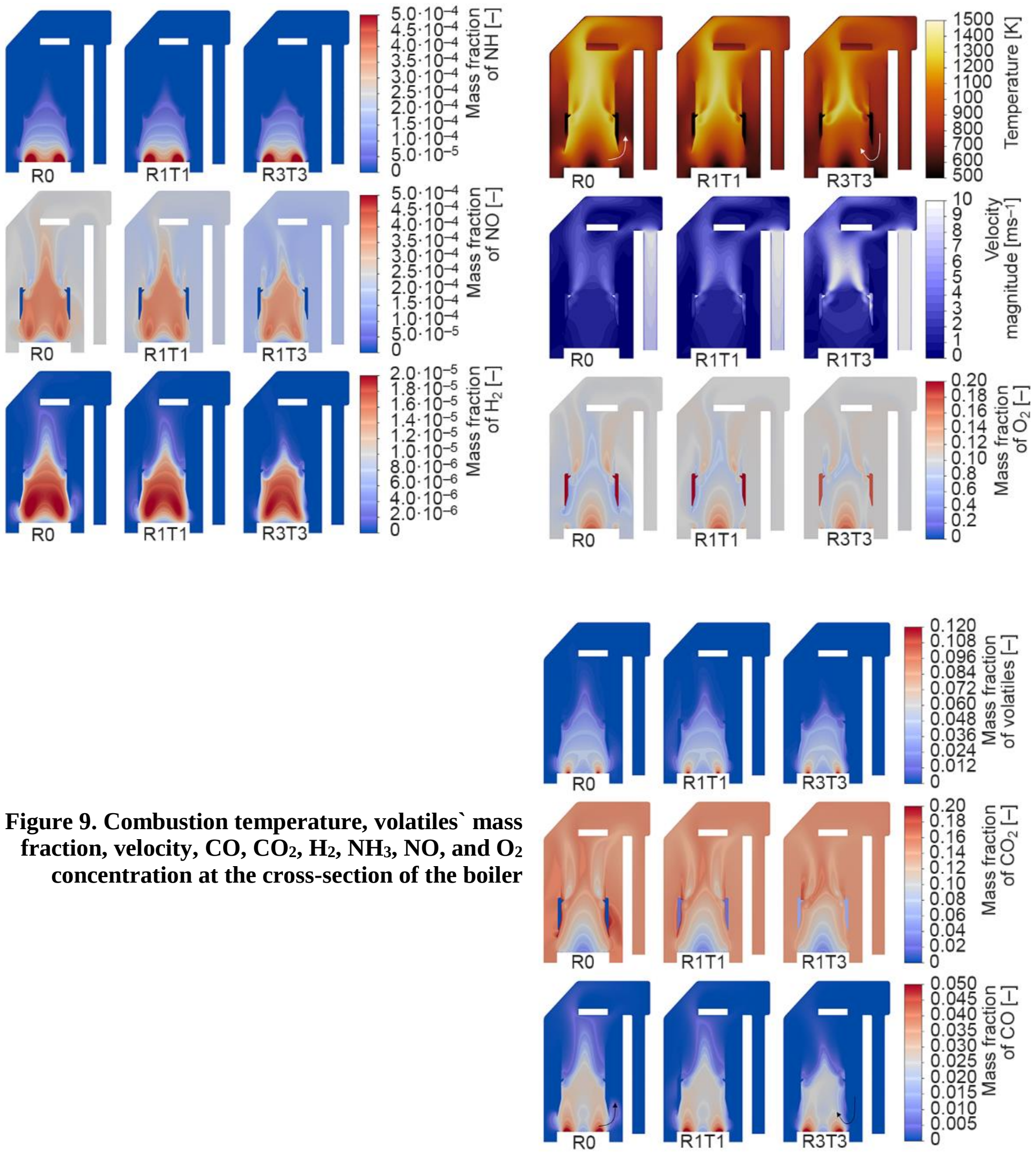

Figure 9. Combustion temperature, volatiles` mass fraction, velocity, CO, CO_2, H_2, NH_3, NO, and O_2 concentration at the cross-section of the boiler

hot-water boiler. An empirical 1-D fuel bed conversion model was used to simulate the solid fuel conversion. The validation of the numerical baseline case R0 showed that, despite the over prediction of temperature, the results were accurate enough to evaluate the different flue gas recirculation scenarios.

First, a numerical simulation was conducted, with the fuel bed boundary conditions coinciding with the normal operation at a nominal heat output of the system. Then, a CFD parametric study was conducted, to study the impact of the 10%, 20%, and 30% RFG addition to the SA stream on the emissions of CO and NO with a fixed air staging strategy. Furthermore, the impact of temperature of the RFG stream was investigated by testing three different temperatures of the RFG stream. Several conclusions were drawn from the results, which indicated the potential benefits of the method.

The scenarios where RFG were added to the SA were beneficial in all cases regarding the CO and NO emissions. Optimally, a reduction of 63% was achieved by adding 30% of RFG to the SA stream at a combined temperature of 518 K. Similarly, a 22% reduction was achieved for the NO emissions.

The highest CO emission levels were predicted for the case R3T1, where the strongest flow of RFG was assumed at a mixture temperature of 342 K. This relatively low temperature, despite the large mass-flow, caused the reactive mixture to be cooled, and therefore lowered the reaction rates of CO oxidation to CO_2. Therefore, for achieving low CO emissions` temperature and RFG the boundary conditions should be chosen carefully, to avoid undercooling of the reactive mixture.

The combined effect of the RFG addition at an elevated temperature caused an increase in velocity at the SA nozzles. For case R3T3 the average velocity of gases leaving the 32 SA nozzles was effectively doubled compared to the baseline case R0. The higher velocity caused better mixing, as more oxygen was transported to the central region of the SA diffuser, and thus improved the CO burnout.

Higher SA nozzle velocities promoted the IFGR effect in the combustion chamber. The NO emissions correlated to the IFGR mass-flow linearly for cases in the same temperature group. A weaker correlation was observed for the change of temperature inside each group of fixed FGR ratio.

Acknowledgment

The authors acknowledge the financial support from the Slovenian Research Agency (Research Core Funding No. P2-0196).

References

[1] Konig, M., *et al*., Combined Removal of Particulate Matter and Nitrogen Oxides from the Exhaust Gas of Small-Scale Biomass Combustion, *Biomass Convers. Biorefinery*, *9* (2019), 1, pp. 201-212
[2] Hodzic, N., *et al*., Influence of Over Fire Air System on NO_x Emissions – An Experimental Case Study, *Therma Science*, *23* (2018), 3, pp. 2037-2045
[3] de Jong W., van Ommen, J. R., *Biomass as a Sustainable Energy Source for the Future: Fundamentals of Conversion Processes*, Wiley, New York, USA, 2014
[4] Kaltschmitt, M., *et al*., *Energie aus Biomasse: Grundlagen, Techniken und Verfahren*, Springer-Verlag Berlin Heidelberg, 2016
[5] Znidarcic, A., *et al*., Surrogate Model for Improved Simulations of small-Scale Sludge Incineration Plants, *Fuel*, *280* (2019), June, 118422
[6] Zadravec, T., *et al*., The Impact of Secondary Air Boundary Conditions on CFD Results in Small-Scale Wood Pellet Combustion, *Fuel, 324* (2022), Part A, 124451
[7] Khodaei, H., *et al*., Air Staging Strategies in Biomass Combustion-Gaseous and Particulate Emission Reduction Potentials, *Fuel Process. Technol.*, *157* (2017), Mar., pp. 29-41
[8] Zadravec, T., *et al*., Influence of Air Staging Strategies on Flue Gas Sensible Heat Losses and Gaseous Emissions of a Wood Pellet Boiler: An Experimental Study, *Renew. Energy*, *178* (2021), Nov., pp. 532-548
[9] Patronelli, S., *et al*., Combustion of Wood-Chips in a Small-Scale Fixed-Bed Boiler: Validation of the Numerical Model Through In-Flame Measurements, *Fuel*, *221* (2018), 1, pp. 128-137
[10] Rajh, B., *et al*., Advanced Modelling and Testing of a 13 MWth Waste Wood-Fired Grate Boiler with Recycled Flue Gas, *Energy Convers. Manag.*, *125* (2016), Oct., pp. 230-241
[11] Brink, A., *et al*., A Simplified Kinetic Rate Expression for Describing the Oxidation of Volatile Fuel-N in Biomass Combustion, *Energy and Fuels*, *15* (2001), 5, pp. 1094-1099

[12] Barroso, G., *et al*., Modelling and Validation of Biomass Combustion in a Screw Burner, *Fuel*, *254* (2019), June, 115672
[13] Manić, N. G., *et al*., Application of Different Turbulence Models for Improving Construction of Small-Scale Boiler Fired by Solid Fuel, *Thermal Science*, *21* (2017), Suppl. 3, pp. S809-S823
[14] Gomez, M. A., *et al.,* Eulerian CFD modelling for biomass combustion, Transient Simulation of an Underfeed Pellet Boiler, *Energy Convers. Manag.*, *101* (2015), Sept., pp. 666-680

Paper submitted: July 11, 2022
Paper revised: November 28, 2022
Paper accepted: December 9, 2022